

Threshold fracture stress of thin ceramic components

Jürgen Malzbender*, Rolf W. Steinbrech

Forschungszentrum Jülich GmbH, IEF-2, 52425 Jülich, Germany

Received 11 March 2007; received in revised form 10 May 2007; accepted 17 May 2007

Available online 27 July 2007

Abstract

Strength is widely used as a design criterion to characterize the mechanical limits of brittle materials. However, depending on the flaw size distribution, measured strength values show considerable scatter. Statistically this spread can be represented for a specific specimen dimension using Weibull statistics with the characteristic strength, Weibull modulus and threshold strength. A comparison of three- and two-parameter Weibull approaches is exemplified using fracture stress results of thin bi-layer ceramic bending specimens taken from solid oxide fuel cell (SOFC) components. Considering statistical parameters and the flaw size limiting thickness of the substrate layer in a SOFC, the three-parameter Weibull statistics is demonstrated to be more appropriate for the fracture characterization of thin ceramic components.

© 2007 Elsevier Ltd. All rights reserved.

Keywords: Fuel cells; Mechanical properties; Fracture; Strength

1. Introduction

Ceramic materials find widespread application as structural and more importantly as functional layers in composite components.¹ However, ceramic materials exhibit brittle behavior and thus thermo-mechanical aspects provide a permanent risk for mechanical integrity and reliability, since the fracture stress of brittle materials usually displays considerable scatter that depends on the defect size distribution. Failure characterization typically relies on statistical approaches. Weibull statistics are used widely to describe the brittle fracture behavior analytically.^{2,3} Based on the “weakest-link hypothesis” it is assumed that the most serious flaw controls the strength.^{4,5} In general, the critical parameters for predicting the fracture behaviour are the specific component dimensions, characteristic strength, Weibull modulus and threshold strength, although often failure of large scale ceramic specimens is described with two-parameter Weibull statistics comprising of characteristic strength and Weibull modulus. The introduction of a threshold stress appears to be especially reasonable for thin ceramic components, where the maximum defect size is limited by the specimen dimensions. In order to exemplify the failure characterization potential of the two- and three-parameter Weibull

relationships, fracture test results of specimens taken from thin planar solid oxide fuel cells (SOFCs) are used.

The operation of SOFC components at relatively high temperatures (~800 °C) and the need for thermal cycles in service make the thermo-mechanical reliability of the applied brittle ceramic materials extremely important. In addition, the effect of scale-up of cells and stacks has to be assessed with respect to mechanical behavior and failure probability of the SOFC components.

A planar SOFC cell consists basically of anode, electrolyte and cathode with additional interfacial functional layers.⁶ Since the predominantly ceramic materials of the layers are rigidly bonded, differences in material properties result in residual stresses which can facilitate component fracture. Such stresses arise from manufacturing, i.e., intrinsic stresses due to co-firing of the cells, from differences in thermal expansion and from thermal/chemical gradients of diffusing species.^{7,8} Additional stresses can be introduced by the final arrangement and fixation of the cells in the SOFC stack and by temperature gradients associated with the actual heating and cooling conditions.

Although investigations of the mechanical properties of SOFC cells have been carried out^{9,10}, the existence of a threshold strength has not been investigated to date. Here, an investigation using biaxial testing of the strength of SOFC half-cells, consisting of anode substrate (~1 mm) and electrolyte (~10 μm), is presented. The analyses take into consideration the layered structure of the half-cells, in particular the effect of the electrolyte layer on stiffness and residual stresses. Statistical assessments

* Corresponding author. Tel.: +49 2461 616964; fax: +49 2561 613699.
E-mail address: J.malzbender@fz-juelich.de (J. Malzbender).

using the two- and three-parameter Weibull distributions are compared. A theoretical limit of the threshold stress is estimated and compared to the experimental value. Implications for the failure probability prediction of large planar SOFC components are discussed.

2. Experimental

Planar SOFCs, fabricated as part of the activities of the R&D fuel cell project at the Forschungszentrum Jülich (FZJ), were used for the preparation of specimens for the mechanical tests. Half-cells without cathode were assessed, since initial investigations showed that the cathode, which possesses a very low stiffness, influenced neither the residual stress nor the composite stiffness significantly.¹⁰ The SOFC half-cells consisted of a thick porous NiO–YSZ anode (~ 1 mm) supporting an anode functional layer ($\sim 5 \mu\text{m}$) and a thin YSZ electrolyte ($\sim 10 \mu\text{m}$). From large half-cells ring-on-ring test specimens ($\sim 24 \text{ mm} \times 24 \text{ mm} \times 1 \text{ mm}$) were machined by laser cutting.

The ring-on-ring bending tests were carried out in an Instron 1362 testing machine following the European standard EN 1288-1. Load–displacement curves provided the raw data for the strength determination of the half-cells. Elastic moduli of anode (97 GPa) and electrolyte (200 GPa) were obtained by depth sensing indentation.^{11,12}

The stress in an isotropic material resulting from ring-on-ring testing can be calculated using linear bending theory^{13,17,15}:

$$\sigma = \frac{3P}{2\pi t^2} \left[(1 + \nu) \ln \left(\frac{r_2}{r_1} \right) + \frac{1 - \nu}{2} \left(\frac{r_2^2 - r_1^2}{r_3^2} \right) \right] \quad (1)$$

where P is the applied force, t the specimen thickness, ν the Poisson ratio and r_1 , r_2 and r_3 are the radii of the load ring, supporting ring and (circular) specimen, respectively. Since square specimens have been tested with the side length L , an equivalent average radius r_{3m} was substituted for r_3 , which can be estimated using^{15,17} $r_{3m} = L(1 + \sqrt{2})/4 \approx 0.6L$. A similar relationship suggested in Ref.¹³ changes the effective diameter by only $\sim 10\%$. Equations which permit a determination of the entire stress field and deformed shape can be found in Ref.¹⁵.

Certain limitations for the use of the ring-on-ring test derived in literature^{13,14} were considered. The linear theory is valid as long as the deflection of the specimen does not exceed a discrete value which depends on the ratio of the loading to supporting ring and is $\sim 1/2$ of the specimen thickness for a ratio of two and ~ 3 for a ratio of five.^{15–17} In order to avoid non-linearities in the load-stress conversion related with large deflection the thickness has to be $t \geq \sqrt{8\sigma_f r_1^2 / 3E}$, where E is the elastic modulus. Since the largest measured fracture stress value was ~ 85 MPa, the calculated value $t \geq 460 \mu\text{m}$ was well below the thickness of the specimens (~ 1 mm).

In the case of a layered composite the effect of the layered arrangement on the residual stress, the neutral axis and flexural rigidity have to be considered.¹⁸ The half-cell specimens break if the fracture stress of the anode is exceeded since the electrolyte is under high compressive residual stress and failure before the anode breaks therefore unlikely.^{10,19} If the bending of the half-

cell specimens is carried out with the free surface of the anode (suffix 1) under tension (compression – sign in the second part of the nominator) a simplified solution with an error $< 3\%$ for the considered materials combination is represented by:

$$\sigma_f = \frac{3P((1 + \nu) \ln(r_2/r_1) + (1 - \nu)/2((r_2^2 - r_1^2)/r_3^2)) \pm 4(\alpha_2 - \alpha_1)t_1 t_2 E_2 \pi T}{2\pi t_1^2} \quad (2)$$

where α is the thermal expansion coefficient, t the thickness and T is the temperature. The strength of SOFC half-cells has been determined using Eq. (2). The electrolyte will change the position of the neutral bending axis, which results for the considered geometry in a strength decrease of $\sim 1\%$, but it also increases the stiffness of the composite by $\sim 3\%$. The main effect of the electrolyte is the residual stress induced in the anode. Based on a misfit in thermal expansion of $2 \times 10^{-6} \text{ K}^{-1}$ and a stress free temperature of 1100°C ¹⁰, a resulting residual stress of -8 MPa in the free surface of the anode was obtained, which has to be added to the strength values.

3. Theory

According to the Weibull statistics⁴, the cumulative failure probability $P(\sigma)$ of a brittle material subjected to a stress σ is given by:

$$P(\sigma) = 1 - \exp \left[- \left(\frac{\sigma - \sigma_u}{\sigma_0} \right)^m \right] \quad (3)$$

where σ_0 is a normalization factor known as the characteristic fracture strength or scale parameter, σ_u the threshold stress or location parameter, below which no failure will occur and m is the Weibull modulus or shape parameter of the distribution, being a measure of strength diversity.

The characteristic strength corresponds to a failure probability of 63.21% and is hence a weak criterion for assessing the reliability of brittle materials. Only the knowledge of characteristic strength, Weibull modulus and threshold strength permits a complete characterization of a material for a discrete specimen dimension and an estimation of the failure probability for a particular stress level. Often σ_u is assumed to be zero in Eq. (3), yielding the two-parameter relation.

The results obtained from both numerical simulations and real data have shown that, as long as sample data are limited in number (~ 40) and the threshold stress is not too large ($\sim \sigma_u < 0.5\sigma_0$), a two-parameter Weibull distribution should be preferred.^{20,21} It has also been demonstrated that an underestimation rather than an overestimation of the threshold stress is more likely, which is an advantage for failure predictions.²²

However, it is important to emphasize that two- and three-parameter Weibull distributions will lead to differences in the estimated stress for a particular failure probability. Obviously, such differences can become even more significant if failure stress predictions are extrapolated from small specimens to large components. Depending on the location of failure initiation, surface or volume defects, the ratio of characteristic fracture strengths is related either to the ratio of stressed surface areas or

volumes, via²³:

$$\left(\frac{\sigma_{0,G_1} - \sigma_u}{\sigma_{0,G_2} - \sigma_u}\right) = \left(\frac{G_1}{G_2}\right)^{-1/m} \quad (4)$$

where G can be either area (A) or volume (V). The statistical parameters of the Weibull distribution are most frequently assessed using linear regression (LR) or the maximum likelihood method (ML).²⁴ Linear regression is a special case of the least-squares method, taking twice the logarithm of Eq. (3), with the slope m and the y-intercept σ_0 . In the LR method the stress values have to be ranked with respect to their individual probability, where the most commonly used expression is²⁴: $P_i(\sigma) = (i - 0.5)/N$. The quality of the fit is usually assessed by the uncertainty in the regression slope m . It has been recognized that the maximum likelihood method is more reliable; however, the use of both distributions to analyze three-parameter Weibull distributions is limited.

In the maximum likelihood method the parameters of the Weibull distribution are determined from the log-likelihood function²⁴:

$$\ln L = \sum_{i=1}^N \ln \left\{ \frac{m}{\sigma_0} \left(\frac{\sigma_i - \sigma_u}{\sigma_0}\right)^{m-1} \exp \left[-\left(\frac{\sigma_i - \sigma_u}{\sigma_0}\right)^m \right] \right\} \quad (5)$$

In the solution a threshold stress is chosen and the Weibull modulus is obtained by iteration until convergence is obtained.²²

For small specimen numbers the Weibull modulus needs to be corrected. As an example a factor of $1 - 1.593145 N^{-1.046958}$ has been suggested.²⁴ For the large specimen number ($N = 180$) analyzed here the factor takes a value of ~ 0.993 , changing the Weibull modulus by only $\sim 0.7\%$.

Various methods have been suggested to estimate the uncertainty of the Weibull parameters. Here standard the deviation, confidence interval (also Bootstrap), coefficient of variance and Akaike information criterion (AIC) are used to assess the quality of the fit (see Appendix A).

4. Results and discussion

Linear regression and maximum likelihood methods were used to analyze 180 experimentally measured fracture stresses of SOFC half-cell specimens, tested in a ring-on-ring setup. A linear regression fit of the two- and three-parameter Weibull distribution to the data is shown in Figs. 1 and 2. Contrary to the three-parameter distribution which yields a threshold stress of ~ 30 MPa, the two-parameter Weibull distribution shows significant

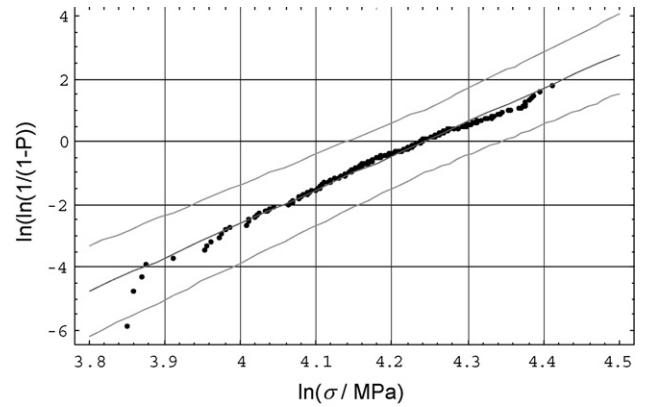


Fig. 1. Weibull plot of $\ln(\ln(1/(1-P)))$ vs. $\ln(\sigma/\text{MPa})$. The lines are a fit of Eq. (5) with $\sigma_u = 0$ (two-parameter Weibull distribution).

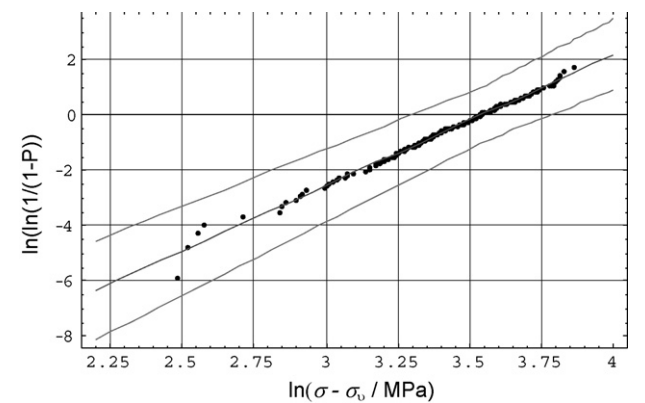


Fig. 2. Weibull plot of $\ln(\ln(1/(1-P)))$ vs. $\ln(\sigma - \sigma_u/\text{MPa})$. The lines are a fit of Eq. (5) with $\sigma_u = 27$ MPa (three-parameter Weibull distribution).

deviation for the data at low fracture stresses. This implies that there are more failures than to be expected in this particular stress range.

The characteristic strength and Weibull modulus as well as the threshold strength for the two- and three-parameter Weibull distribution are given in Table 1. As reported in literature²³ the three-parameter distribution leads to a lower Weibull modulus if fitted to the same set of experimental data.

In addition, the table contains the standard deviation of σ_u , σ_0 and m . The standard deviation of the fracture stress for a discrete probability σ_f is a result of the combined standard deviation in σ_u , σ_0 and m . The standard deviation is compared to the limits of the confidence intervals determined on the basis of the industrial standard in Table 2. The use of the standard deviation can only be considered as an approximation, since it assumes a symmetric distribution. The standard deviation implies that

Table 1
Results of the linear regression (LR) and maximum likelihood method (ML) and fracture stress σ_f for a failure probability of 10^{-3} and 10^{-6}

Method	σ_u (MPa)	σ_0 (MPa)	m	σ_f (MPa) for $P = 10^{-3}$	σ_f (MPa) for $P = 10^{-6}$
LR, 2-p.	0	62 ± 1	11 ± 1	33 ± 3	17 ± 3
LR, 3-p.	27 ± 1	61 ± 1	4.7 ± 0.3	41 ± 2	30 ± 2
ML, 2-p.	0	62 ± 1	10 ± 1	31 ± 3	16 ± 3
ML, 3-p.	26 ± 1	61 ± 1	4.8 ± 0.4	40 ± 2	29 ± 2

Table 2

A comparison of the standard deviation and confidence intervals for the results of the linear regression (LR) and maximum likelihood method (ML)

Method	$s(\sigma_0)$ (MPa)	$s(m)$	C_u, C_l	D_u, D_l	$C_u, C_l/s(\sigma_0)$	$D_u, D_l/s(m)$
LR, 2-p.	± 1	± 1	± 1	± 1	1	1
LR, 3-p.	± 1	± 0.3	± 1	± 0.6	1	1/2
ML, 2-p.	± 1	± 1	± 1	± 1	1	1
ML, 3-p.	± 1	± 0.4	± 2	± 0.8	1	1/2

$\sim 68\%$ of the data should be within this limit, $\sim 95\%$ within twice the limit. Comparing the 95% confidence interval with the standard deviation shows good agreement for the strength and the two-parameter Weibull modulus.

The three-parameter bootstrap Weibull modulus confidence interval has been determined in addition to the confidence interval based on the industrial standard. For 2000 re-sampled data sets taken from the experimentally determined fracture strength as outlined in the appendix, the bootstrap confidence interval agreed with a value of ± 1 with the confidence interval based on the industrial standard.

The confidence intervals based on the industrial standard are displayed along with the experimental data in Figs. 1 and 2. For the two-parameter Weibull distribution the data at low stresses come close to the limit, whereas the data for the three-parameter Weibull distribution are all well within the limits set by the confidence interval. Also the standard deviation, which is lower for the three-parameter distribution, reflects the smaller deviation of data to fit. As a theoretical limit of the coefficient of variation it has been suggested³² that $c_v = 1.272/(m + 0.525)$. Comparing this limit to the value obtained above results in a ratio of 0.9997 for the maximum likelihood results of three-parameter Weibull distribution and 1.777 for the two-parameter distribution.

When comparing the two- with three-parameter description, the latter should demonstrate a significantly better fit to justify the additional parameter. The AIC is 624 for the two-parameter and 623 for the three-parameter distribution, if the characteristic strength and Weibull modulus are determined on the basis of the maximum likelihood method. The values are 626 and 623 if linear regression is used to determine the strength and Weibull modulus. Hence the AIC is always higher for the two-parameter distribution, supporting the validity of the three-parameter description. Hence, all uncertainty assessment parameters suggest that the three-parameter Weibull distribution is a better description of the experimental data.

Table 1 also contains fracture stress σ_f for a failure probability of 10^{-3} and 10^{-6} . Note that, especially for a failure probability 10^{-6} , the use of a two-parameter distribution leads to a significant underestimation of the critical stress, with severe implications for the proof testing of such thin ceramics components.

The anode size in a SOFC stack is usually significantly larger than the specimen size. Generally, a larger size results in a lower characteristic strength described by Eq. (5). The strength is determined here using a ring-on-ring test geometry. Hence, it is necessary to determine the deformed volume in this test. The effective volume can be determined from integration of the stress over the entire specimen volume. Explicit solutions exist

for three- and four-point bending.²⁵ The deformed volume in a ring-on-ring test can be estimated by¹³

$$V_{\text{eff,specimen}} = \left(\frac{(2\pi r_1^2)t}{2(m+1)} \right) \left(1 + \frac{44(1+\nu)m+5}{3(m+1)m+2} \right) \times \left(\frac{r_2-r_1}{2r_1r_3} \right)^2 \frac{8r_3^2(1+\nu)+4(r_2-r_1)^2(1-\nu)}{(3+\nu)(1+3\nu)} \quad (6)$$

For the considered loading geometry and Weibull moduli the error in using Eq. (6) is only $\sim 5\%$.¹³ Since using this relationship a determination of the entire volume under tensile stress is possible, hence not being specific anymore for the particular bending situation and eliminating the effect of the stress gradient during the test, the characteristic strength of an anode in cell size ($V_{\text{eff,cell}} = \text{length} \times \text{width} \times \text{thickness}$) can be determined from Eq. (6) in combination with Eq. (4). The fracture stress for a failure probability of 10^{-6} for anode in cell size (100 mm \times 100 mm) can also be calculated using Eq. (6) in combination with the data given in Table 1. For the LR method a value of 9 MPa is obtained for the two-parameter distribution and 28 MPa for the three-parameter distribution. In the case of the ML method the values are by 8 and 27 MPa, respectively. This shows even larger fracture stress differences obtained for large cells in the case of two- and three-parameter distributions.

Additional information on the existence of a threshold stress for thin components can be obtained from the fracture toughness. The necessary criterion for fracture is that²⁶:

$$K_{\text{IC}} = F\sigma\sqrt{\pi c} \quad (7)$$

where K_{IC} is the fracture toughness, σ the applied stress and c the defect size. The function F is a function of the ratio of defect size to specimen thickness/diameter and depends on the loading situation. It is not far fetched to assume that as long as no processing related cracks are induced the defects are related to the structure of the material. The anodes are porous to permit hydrogen gas to reach the electrolyte layer during high temperature operation. The maximum size of pores is limited by the thickness of the specimen. In the case of the bending of a plate^{27,28} $F = \sqrt{(1+\nu)}/\sqrt{(3+\nu)}$, yielding for $\nu = 0.3$ a value of $F \sim 0.63$. In the estimate of the threshold stress an SOFC anode fracture toughness of 1.2 MPa m^{1/2} is used.²⁹ Based on these data a threshold stress of ~ 34 MPa is estimated, which is in agreement with the threshold value determined from the three-parameter Weibull distribution.

This threshold stress depends only on the thickness and will be the same for large cells in a SOFC stack. Note, however, that as mathematically described by Eq. (7) the threshold stress in the tensile loading situation of a planar SOFC stack is reduced by a factor of $\sim 1/0.63$, yielding a value of only ~ 21 MPa.

Similarly, the threshold strength of the electrolyte can be estimated, since the maximum defect size is limited to the thickness of the electrolyte. The fracture toughness, in this case, is given by³⁰:

$$K_{IC} = g(E_1, E_2)\sigma\sqrt{t} \quad (8)$$

where $g(E_1, E_2)$ is as function of E_1 and E_2 , the elastic moduli of electrolyte and anode, and t the thickness of the electrolyte. For the considered material combination, $g(E_1, E_2)$ takes a value of 0.43.³⁰ In the calculation of the threshold stress a SOFC electrolyte fracture toughness of $2 \text{ MPa m}^{1/2}$ is used.²⁹ The threshold strength is then ~ 370 MPa for a $10 \mu\text{m}$ electrolyte and ~ 520 MPa for a $5 \mu\text{m}$ electrolyte thickness. The threshold strength of the electrolyte will be further enhanced by the residual stress which is approximately -560 MPa for a $10 \mu\text{m}$ electrolyte at RT and ~ 280 MPa at a typical operation temperature of 800°C .¹⁹

5. Conclusions

An investigation on the strength of SOFC half-cells has been presented. The results of statistical analyses of the strength data using the two- and three-parameter Weibull distributions are compared. Various methods for assessing the uncertainty are presented and discussed with respect to the resulting strength data. The fracture stress for failure probabilities and larger anode sizes as typically used in SOFC stacks are estimated. Especially for large cells, fracture stress predictions based on two-parameter distributions can underestimate the critical stress. A theoretically estimated threshold stress for specimens of limited thickness compares well with the experimental value (~ 30 MPa). A three-parameter Weibull statistics appears to be more appropriate for the fracture of thin ceramic components.

Acknowledgments

The work partly supported financially by the EU under the project “Realising Reliable, Durable, Energy Efficient and Cost Effective SOFC Systems” (Real-SOFC). The authors would like to thank Dr. H.P. Buchkremer and J. Mertens for providing the SOFC material.

Appendix A. Uncertainty assessment

The standard deviations of the strength $s(\sigma_0)$ and Weibull modulus $s(m)$ have been defined as³¹ $s(\sigma_0) = \sigma_0/(m\sqrt{N})$ and $s(m) = m/\sqrt{N}$.

The upper C_u and lower limit C_l of the confidence interval for the characteristic strength can be determined via²⁴: $C_u = (\sigma_0 - \sigma_u) \exp[-t_u/m]$ and $C_l = (\sigma_0 - \sigma_u) \exp[-t_l/m]$, where

t_u and t_l are the upper and lower limiting factor for the confidence interval which depend on the confidence limit and the specimen number. Tabulated values and formulas are available²⁴. For the considered specimen number and a confidence level of 95% the values are $t_u \sim -0.178$ and $t_l \sim 0.183$.

For the Weibull modulus the respective formula for the upper and lower limit are $D_u = m/l_u$ and $D_l = m/l_l$, where l_u and l_l are the upper and lower limiting factor for the confidence interval which depend again on the confidence limit and the specimen number. Again, tabulated values and formulas are available. For the considered specimen number and a confidence level of 95% the values are $l_u \sim 0.879$ and $l_l \sim 1.134$.

As an alternative method for determining the confidence interval, a bootstrap re-sampling procedure can be used, which allows the empirical distribution function to be obtained from random sampling. Bootstrap confidence intervals are obtained in the following way: a bootstrap sample is obtained by randomly sampling, N times (here 180), with replacement, from the original data. The procedure is repeated K times (here 2000) and a large number of independent bootstrap samples are obtained. Each bootstrap sample is analysed using Weibull statistics and the confidence interval is obtained from the resulting characteristic strength values of the bootstrap samples.

Another model to assess the width of the strength distribution is the coefficient of variance, which is generally defined as³²: $c_v = \left[1/N \left(\sum_{i=1}^N \{(\sigma_i - \bar{\sigma})^2\}\right)\right]^{1/2}$, where the mean of the distribution is $\bar{\sigma} = \sigma_0 \Gamma \left[1 + (1/m)\right]$, here Γ is the gamma function. Note, although coefficient of variance and standard deviation are generally linked this is not the case with the definition used in Section 4.

It is easier to fit a data set using a complex model with more parameters than a simple one with only few parameters. The Akaike information criterion (AIC)^{33,34,20,22} represents a useful heuristic measure to compensate the additional parameters. The AIC can be used to assess the distance between the true and estimated distributions, and is defined as: $\text{AIC} = -2(\ln \hat{L} - k)$, where $(\ln \hat{L})$ is the maximum log-likelihood of a given model and k is the number of fitting parameters. A confidence level differences of $\sim 5\%$ corresponds to differences in AIC values of around 1.5–2.²⁰ The three-parameter Weibull distribution should demonstrate a significantly better fit to justify the additional parameter.

References

- Advances in Solid Oxide Fuel Cells: A Collection of Papers Presented at the 29th International Conference on Advanced Ceramics and Composites, 23–28 January, 2005, Cocoa Beach, Florida, Ceramic Engineering and Science Proceedings, vol. 26, No. 4, 2006.
- Wachtman, J. B., *Mechanical Properties of Ceramics*. Wiley, New York, 1996.
- Weiderhorn, S. M. and Fuller Jr., E. R., Structural reliability of ceramic materials. *Mater. Sci. Eng.*, 1985, **71**, 169–186.
- Weibull, W., A statistical theory of the strength of materials. *Proc. R. Swed. Inst. Eng. Res.*, 1939, **151**, 1–45.
- Weibull, W., A statistical distribution function of wide applicability. *J. Appl. Mech.*, 1951, **18**, 293–297.
- Tietz, F., Thermal expansion of SOFC materials. *Ionics*, 1999, **5**, 129–139.

7. Hendriksen, P. V., Carter, D. J. and Mogensen, M., Dimensional instability of doped lanthanum chromites in an oxygen pressure gradient. *Proc. Electrochem. Soc.*, 1995, **951**, 934–943.
8. Adamson, M. T. and Travis, R. P., Comparison of stress generating mechanisms in a planar solid oxide fuel cell stack. *Proc. Electrochem. Soc.*, 1997, **18**, 691–699.
9. Atkinson, A. and Selcuk, A., Mechanical properties of ceramic materials for solid oxide fuel cells. *Electrochem. Soc. Proc.*, 1997, **18**, 671–680.
10. Malzbender, J., Steinbrech, R. W. and Singheiser, L., Failure probability of solid oxide fuel cells. *Ceram. Eng. Sci. Proc.*, 2005, **26/4**, 293.
11. Malzbender, J., den Toonder, J. M. J., Balkenende, A. R. and de With, G., A methodology to determine the mechanical properties of thin films, with application to nano-particle filled methyltrimethoxysilane sol-gel coatings. *Mater. Sci. Eng. R.*, 2002, **36**, 47.
12. Malzbender, J., Wakui, T., Steinbrech, R. W. and Singheiser, L., Deflection of planar solid oxide fuel cells during sealing and cooling of stacks. *Fuel Cell*, 2006, **2**, 123.
13. Salem, J. A. and Powers, L., Guidelines for the testing of plates. Proceedings 27th International Cocoa Beach Conference. *Ceram. Eng. Sci. Proc.*, 2003, **24(4)**, 357–364.
14. ASTM Standard C 1499 – 05, Standard test method for monotonic equibiaxial flexure strength of advanced ceramics at ambient temperature, ASTM, 2004.
15. Schmitt, R. W., Blank, K. and Schönbrunn, G., Experimentelle spannungsanalyse zum doppelringverfahren. *Sprechsaal*, 1983, **116**, 397–405.
16. Kao, R., Perrone, N. and Capps, W., Large deflection solution of the coaxial-ring-circular-glass-plate flexure problem. *J. Am. Ceram. Soc.*, 1971, **54**, 566–571.
17. Deutsche Norm, Bestimmung der Biegefestigkeit von Glas, DIN 1288-1, 2000.
18. Malzbender, J. and Steinbrech, R. W., Mechanical properties of multilayered composites determined using bending methods. *Surf. Coat. Technol.*, 2004, **176**, 165.
19. Fischer, W., Malzbender, J., Blass, G. and Steinbrech, R. W., Residual stresses in planar solid oxide fuel cells. *J. Power Sources*, 2005, **150**, 73.
20. Lu, C., Danzer, R. and Fischer, F. D., Influence of threshold stress on the estimation of the Weibull statistics. *J. Am. Ceram. Soc.*, 2002, **85**, 1640–1642.
21. Fok, S. L., Mitchell, B. C., Smart, J. and Marsden, B. J., A numerical study on the application of the Weibull theory to brittle materials. *Eng. Fract. Mech.*, 2001, **68**, 1171–1179.
22. Smart, J., Mitchell, B. C., Fok, S. L. and Marsden, B. J., The effect of the threshold stress on the determination of the Weibull parameters in probabilistic failure analysis. *Eng. Fract. Mech.*, 2003, **70**, 2559–2567.
23. Trustum, K. and Jayatila, A. D., On estimating the Weibull modulus for a brittle material. *J. Mater. Sci.*, 1979, **14**, 1080–1084.
24. Deutsche Industrie Norm DIN EN 843-5.
25. Chao, L. Y. and Shetty, D. K., *J. Am. Ceram. Soc.*, 1991, **74**, 333.
26. Tada, H., Paris, P. C. and Irwin, G. R., *The Stress Analysis of Cracks Handbook (3rd ed.)*. ASME Press, 2000.
27. Hui, C. Y. and Zehnder, A. T., A theory of thin plates subjected to bending and twisting moments. *Int. J. Fract.*, 1993, **61**, 211–229.
28. Dirgantara, T. and Aliabadi, M. H., Stress intensity factors for cracks in thin plates. *Eng. Fract. Mech.*, 2002, **69**, 1465–1486.
29. Malzbender, J., Steinbrech, R. W. and Singheiser, L., Determination of the interfacial fracture energies of cathodes and glass ceramic sealants in a planar solid-oxide fuel cell design. *J. Mater. Res.*, 2003, **18**, 929–934.
30. Beuth Jr., J. L., Cracking of thin bonded films in residual tension. *Int. J. Solids Struct.*, 1992, **29**, 1657–1675.
31. de With, G., *Structure, Deformation and Integrity of Materials*. Wiley, Weinheim, 2006.
32. Gong, J. and Li, Y., Relationship between the estimated Weibull modulus and the coefficient of variation of the measured strength for ceramics. *J. Am. Ceram. Soc.*, 1999, **82**, 449–452.
33. Akaike, H., On entropy maximization principle. In *Applications of Statistics*, ed. P. R. Krishnaiah. North-Holland, Amsterdam, The Netherlands, 1977, pp. 27–41.
34. Sakamoto, Y., Ishiguro, M. and Kitagawa, G., *Akaike Information Criterion Statistics*. Reidel, Dordrecht, The Netherlands, 1983.